View metadata, citation and similar papers at core.ac.uk

brought to you by CORE

provided by Elsevier - Publisher Connector

Biochimica et Biophysica Acta 1828 (2013) 1357–1364

Contents lists available at SciVerse ScienceDirect

Biochimica et Biophysica Acta

journal homepage: www.elsevier.com/locate/bbamem

The electrical response of bilayers to the bee venom toxin melittin: Evidence for transient bilayer permeabilization

Gregory Wiedman [a], Katherine Herman [a], Peter Searson [a,*], William C. Wimley [b,*], Kalina Hristova [a,*]

[a] Department of Materials Science and Engineering, Johns Hopkins University, Baltimore, MD 21218, USA
[b] Department of Biochemistry, Tulane University, New Orleans, LA 70112, USA

ARTICLE INFO

Article history:
Received 5 November 2012
Received in revised form 9 January 2013
Accepted 28 January 2013
Available online 4 February 2013

Keywords:
Melittin
Peptide
Pore
Impedance spectroscopy
Protein–lipid interactions

ABSTRACT

Melittin is a 26-residue bee venom peptide that folds into amphipathic α-helix and causes membrane permeabilization via a mechanism that is still disputed. While an equilibrium transmembrane pore model has been a central part of the mechanistic dialogue for decades, there is growing evidence that a transmembrane pore is not required for melittin's activity. In part, the controversy is due to limited experimental tools to probe the bilayer's response to melittin. Electrochemical impedance spectroscopy (EIS) is a technique that can reveal details of molecular mechanism of peptide activity, as it yields direct, real-time measurements of membrane resistance and capacitance of supported bilayers. In this work, EIS was used in conjunction with vesicle leakage studies to characterize the response of bilayers of different lipid compositions to melittin. Experiments were carried out at low peptide to lipid ratios between 1:5000 and 1:100. The results directly demonstrate that the response of the bilayer to melittin at these concentrations cannot be explained by an equilibrium transmembrane pore model.

© 2013 Elsevier B.V. All rights reserved.

1. Introduction

Membrane-active peptides have many potential applications in medicine and biotechnology [1,2]. For example, the design or discovery of peptides that self-assemble into multimeric, membrane-spanning pores could lead to advances in biosensor platforms [3]. Yet peptides that are known to form such explicit pore structures are rare, and the lack of knowledge about the molecular mechanism of pore formation is a roadblock to their rational design or engineering. The best studied membrane permeabilizing peptide is the bee venom toxin melittin [4]. The basic architecture of melittin is well-described [4–6]. It is a cationic 26-residue peptide with a net charge of +6 that partitions strongly into membranes and folds into an amphipathic α-helix. Formation of melittin's helical secondary structure, which is divided into two independent segments by a critical central proline residue at position 14 [7], is tightly coupled to membrane binding because of the strong interaction between the non-polar face of the helix and the lipid hydrocarbon [8,9].

Once it has folded and partitioned into the membrane, melittin causes membrane destabilization and permeabilization by a mechanism that is still disputed [10,11]. Some experiments suggest that melittin self-assembles into a "toroidal" pore [12–15]; either with extended helices spanning the entire bilayer [12] or with helices bent at the central proline residue, spanning half of the membrane thickness as a hairpin [16]. Given that the melittin helix is the appropriate length to span a membrane and is strongly amphipathic, it is easy to imagine and to model transmembrane pores [12,13,15–18]. However, under many experimental conditions melittin in bilayers is predominantly monomeric and interfacially bound [9,10,19–21], which contradicts the pore models. Perhaps more importantly, some experiments [22], including our own [18,21,23], suggest that membrane permeabilization by melittin is a transient phenomenon that occurs only immediately after addition of melittin, and that the "pore" state does not persist at equilibrium.

There are multiple reasons for the current lack of understanding of membrane permeabilization by melittin and similar peptides. First, the details of bilayer permeabilization are dependent on many experimental factors, including lipid composition, ionic strength, temperature, bilayer hydration, and more [11,15,22–28]. For some membrane destabilizing peptides, there may be more than one relevant mechanism of action, depending on the experimental conditions [11,13,27]. For example, melittin's leakage mechanism is very different in fully anionic bilayers compared to zwitterionic bilayers [11]. Likewise, melittin can transition from its typical surface bound state into a transmembrane state when the bilayer hydration is decreased [13]. Second, the mechanism of membrane permeabilization by melittin depends on the peptide concentration. At high melittin concentration, size-independent leakage of macromolecules from vesicles, and changes in light scattering from vesicles support the idea of large-scale membrane disruption, or detergent-like membrane solubilization [11,14,24,28,29]. Solubilization-like phenomena may mimic pore-formation in some

* Corresponding authors. Tel.: +1 410 516 8939.
E-mail addresses: searson@jhu.edu (P. Searson), wwimley@tulane.edu (W.C. Wimley), kh@jhu.edu (K. Hristova).

0005-2736/$ – see front matter © 2013 Elsevier B.V. All rights reserved.
http://dx.doi.org/10.1016/j.bbamem.2013.01.021

experiments [28,30,31], which may explain reports that membrane-spanning melittin structures exist at very high peptide concentration, such as a peptide-to-lipid ratio (P:L) of 1:10 [30]. The relevance of experiments done at very high peptide:lipid ratios, where detergent-like properties are dominant, to the mechanism of action at much lower peptide concentrations, such as we report here, is unknown. Third, there are limited experimental tools to probe the bilayer's functional response to melittin and each method emphasizes different aspects of the process, adding to the uncertainty in mechanism. Vesicle leakage assays are the most frequently used functional assay for pore-forming peptides. However, they typically measure the integrated dissipation of concentration gradients of large (>10 Å) analytes through the bilayers and do not directly measure the response of the bilayer in real time. On the other hand, electrophysiological planar bilayer studies [32,33] directly monitor the bilayer's response to peptides in real time, but are generally carried out under conditions where the peptide to lipid ratio in the membrane is unknown.

Here we use electrochemical impedance spectroscopy (EIS) and vesicle leakage studies in parallel to probe the bilayer response to melittin. EIS is a technique that can reveal details of the molecular mechanisms of peptide activity that are not accessible in lipid vesicle experiments, as it yields direct, real-time measurements of the resistance and capacitance of supported bilayers [34–40]. It is highly sensitive to the passage of small ions, and can thus detect small pores or small disruptions in the bilayer structure. Thus, EIS can be used to probe the low P:L concentration regime. Importantly, the bound P:L ratios used in EIS measurements are under direct experimental control. Furthermore, we have shown that we can vary the lipid composition of the bilayers used in EIS without compromising the bilayer structure or electrical properties [34–36,38,39]. The EIS results presented here for surface-supported bilayers of three different lipid compositions are compared directly to vesicle leakage results and demonstrate that, under the conditions studied here, the response of the bilayer to melittin cannot be explained by equilibrium transmembrane pore models.

2. Materials and methods

The melittin used in this study was purchased from Enzo Life Science International Inc. A stock was prepared in methanol and was stored in 4 °C. Alamethicin was purchased from Sigma Aldrich. Lyophilized powders of 1-palmitoyl-2-oleoyl-*sn*-glycero-3-phosphocholine (POPC), 1-palmitoyl-2-oleoyl-*sn*-glycero-3-phosphoglycerol (POPG), and cholesterol (Chol) were purchased from Avanti and were dissolved in chloroform for use. Indium Gallium eutectic was obtained from Alfa Aesar. The fluorescent dye and quencher, 8-aminonapthalene-1,3,6 trisulfonic acid (ANTS) and p-xylene-bis-pyridinium bromide (DPX) were purchased from Invitrogen Life Technologies. Triton 100-X was obtained from Fischer Scientific. Potassium chloride (KCl), Sodium phosphate (NaH_2PO_4, Na_2HPO_4), HEPES buffer, and all solvents were purchased from Sigma-Aldrich.

2.1. Vesicle preparation

Lipid vesicles were formed by first dissolving lipids in chloroform at 25 mg/mL in a glass vial. The solvent was evaporated under nitrogen for 15 min and the sample was dried under vacuum for at least 30 min. For the leakage experiments, a solution containing 12.5 mM ANTS and 45 mM DPX in 5 mM HEPES buffer, pH 7.4, was added to the lipids and the solution was vortexed to form multilamellar vesicles. Unilamellar vesicles (with and without encapsulated ANTS/DPX) of 0.1 μm diameter were formed by extruding the vesicles at least ten times through a 0.1 μm Nucelopore polycarbonate filter. Vesicles with encapsulated ANTS and DPX were separated from the free dyes on a Sephadex column. The vesicles were stored at 4 °C.

2.2. Bilayer preparation

Bilayers were prepared using Langmuir Blodgett (LB) deposition and vesicle fusion as described in previous work [34–42]. The bilayers consisted of either (i) 100% POPC in both leaflets, (ii) 75% POPC and 25% Cholesterol in both leaflets, or (iii) 90% POPC + 10% POPG in the top leaflet and 100% POPC in the bottom leaflet. The bilayers were constructed on a polymer cushion by incorporating 5.9 mol% DSPE-PEG2K into the lower (LB) leaflet of the bilayers [35,43].

Pieces of (111) silicon were cut and washed with isopropanol (IPA), acetone, IPA and then treated with a piranha etch solution (34% hydrogen peroxide and 66% sulfuric acid). Chloroform solutions of 1 mg/mL (POPC or POPC + Chol with 5.9% PEG2K-DSPC) were deposited onto the surface of a NIMA Langmuir Blodgett Trough. After solvent evaporation, the lipids were compressed to a final surface pressure of 32 mN/m for POPC and 32.5–33 mN/m for POPC/Chol. Immersed silicon pieces were withdrawn at a speed of 15 mm/s, maintaining a constant surface pressure, in order to deposit a monolayer of the desired lipid composition. A Teflon electrochemical cell was clamped to the surface of the silicon with a rubber o-ring in contact with the surface. To prepare a bilayer, 450 μL of a vesicle solution in 10 mM sodium phosphate and 100 mM potassium chloride pH 7.0 (prepared as described above) was deposited onto the area defined by the o-ring. After 1 h, 10 mL of the buffer solution was added to the electrochemical cell on top of the vesicle solution and allowed to sit for up to 24 h before measurements. A hydrofluoric acid etch solution (25% HF) was applied via cotton swab to an exposed piece of the silicon. After 1 min, the excess was removed and an Indium Gallium eutectic was deposited onto the etched surface with the blunt end of the swab.

2.3. Leakage assays

Leakage assays were performed following established protocols [44]. ANTX and DPX were co-encapsulated in the vesicles as described [45,46]. ANTS/DPX containing vesicles (1 mM lipid) were added to a quartz cuvette and the fluorescence was recorded using a Horiba Jobin Yvon FluoroLog fluorometer. After an initial reading was taken, different concentrations of peptide were added to the solution from a concentrated stock solution. The peptides were added with a glass syringe and the peptide addition was immediately followed by 10 cycles of pipette aspiration to allow for mixing. The samples were excited at a wavelength of 355 nm and the fluorescence at 520 nm was recorded for at least 10 min. Afterwards, 50 μL of 10% Triton 100-X was added to fully lyse the vesicles. The amount of leakage due to peptide interaction with the membrane was calculated as:

$$\text{Fractional Leakage} = \frac{I_{peptide} - I_{background}}{I_{final} - I_{background}} \quad (1)$$

where $I_{peptide}$ is the maximum fluorescence measured upon peptide addition, $I_{background}$ is the background fluorescence prior to peptide addition, and I_{final} is the fluorescence after Triton addition. Kinetic traces were obtained by recording the fluorescence intensity every second for up to 15 min.

2.4. Electrochemical impedance spectroscopy

Electrochemical impedance spectroscopy (EIS) was performed using a three electrode electrochemical cell and a Solartron 1286/1255 Electrochemical Interface/Frequency Response Analyzer. An Ag/AgCl reference electrode and a Pt counter electrode were placed into contact with the buffer solution in the cell and connected to the impedance analyzer, while the silicon electrode served as the working electrode. A 20 mV rms perturbation was applied to the cell at zero DC bias (0.0 V vs. Ag/AgCl). Impedance spectra were measured over the frequency range from 10^5 to 1 Hz. Spectra were recorded every 2 min

continuously for one hour. In some cases, additional measurements were performed every hour for up to 16 h. Fits to an ideal circuit were performed using the Zplot software from Scribner. The rest of the data analysis was performed using Igor from WaveMetrics. Individual EIS spectra were analyzed based on fitting to the ideal circuit shown elsewhere [38,39]. In the equivalent circuit, R_{ct} and C_p represent the resistance and the capacitance of the solution-semiconductor interface; R_m and C_m represent the resistance and the capacitance of the bilayer. R_s represents the series resistance of the bulk electrolyte.

As bilayers can have variable initial resistance, R_0, the ratio R_m/R_0 was calculated following peptide addition. For kinetic analysis, the changes in normalized membrane resistance R_m/R_0 were fit to the following equation:

$$\frac{R_m(t)}{R_0} = y + Ae^{-\left(\frac{t-t_0}{\tau}\right)}. \quad (2)$$

In this equation the time constant (τ) was the fitted parameter. The constant t_0 was the time at which the lowest normalized resistance was observed after the initial drop in the case of melittin, or 0 in the case of alamethicin. The offset y was the normalized membrane resistance after 30 min, and A was the difference between the values of the normalized membrane resistance at t_0 and after 30 min.

3. Results

3.1. Response of POPC/Chol bilayers to melittin

First, we investigated the effect of melittin on POPC/Chol bilayers; a lipid composition often used to mimic mammalian cell membranes. The lower leaflet was composed of 25% Chol, 69.1% POPC, and 5.9% DSPE-PEG2K. The last component, DSPE with PEG of molecular weight 2000 covalently attached to its headgroup, was added such that the PEG chains provide a cushion to support the bilayer [35]. The vesicles used in the fusion step were composed of 75% POPC and 25% cholesterol. The initial membrane resistance (R_m) values were $1.71\times10^4 \pm 6.3\times10^3$ Ω cm^2, obtained by fitting the impedance spectra to an equivalent circuit model [38,39]. The initial capacitance value was 0.93 ± 0.12 μF/cm^2 corresponding to a bilayer thickness of 3.8 ± 0.5 nm, assuming a relative permittivity of 4 [38–41].

After bilayer formation and initial impedance measurements, melittin was added to the buffer in the chamber, without removing excess vesicles, as described in previous work [34,37]. This procedure allows us to perform experiments at a well-defined peptide to lipid ratio. Three different melittin:lipid ratios were used, 1:200, 1:500 and 1:1000. Impedance spectra were collected every two minutes after peptide addition and were fitted to the equivalent circuit [38,39], yielding membrane capacitance and resistance as a function of time. Fig. 1a shows the normalized membrane resistance, R_m/R_0, as a function of time, and Fig. 1c shows the membrane capacitance as a function of time. Results shown are the averages from at least three independent experiments ($N \geq 3$). The average standard errors in the measurements are shown in Fig. 1a and c at the end of the curves.

As seen in Fig. 1a, the bilayer resistance dropped abruptly after the addition of melittin, consistent with many observations that melittin is a potent membrane destabilizing peptide. However the resistance drop was followed, unexpectedly, by an exponential recovery to a steady state value that was 60–80% of the initial resistance. The final resistance was not strongly dependent on peptide concentration. The time constants for this recovery phase were obtained by fitting the transient membrane resistance to a single exponential (Eq. (2)). The time constants for recovery were on the order of 10 min. The bilayer capacitance showed a small decrease in the first measurements after peptide addition that was reproducible, but was similar in magnitude to the experimental uncertainties. This may suggest a slight thickening of the bilayer due to peptide binding. However, the capacitance did not change any more over the remaining course of the 60 min measurement

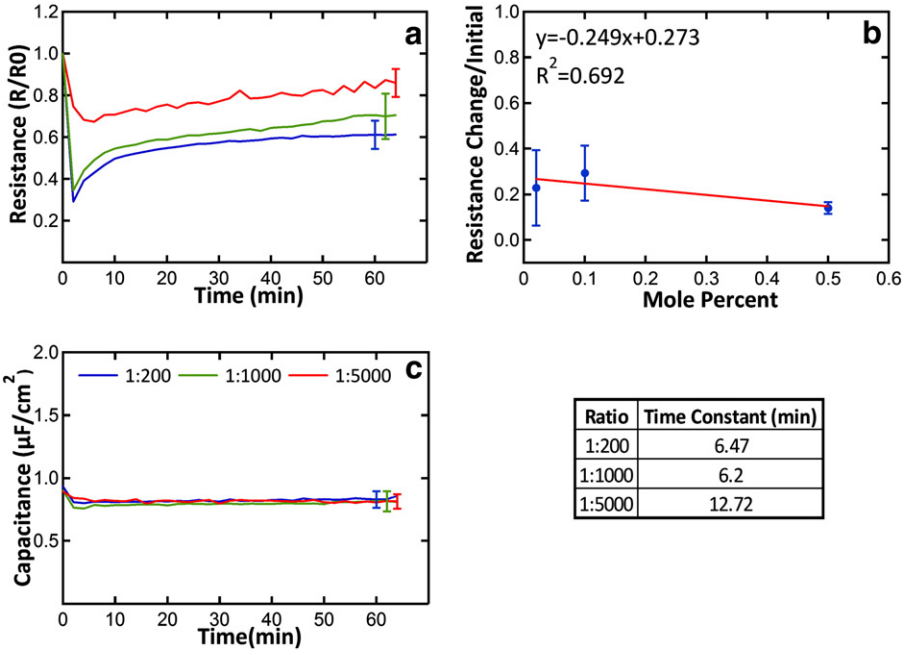

Ratio	Time Constant (min)
1:200	6.47
1:1000	6.2
1:5000	12.72

Fig. 1. EIS response of POPC/Chol bilayers to melittin. The bilayer composition was 25% Chol, 69.1% POPC, and 5.9% DSPE-PEG2k in the lower leaflet and 75% POPC and 25% Chol in the top leaflet. Melittin was added at peptide to lipid ratios of 1:200, 1:1000, and 1:5000, calculated based on a final lipid concentration of 65 μM in the impedance chamber. Panel a shows the normalized change in resistance $R_m(t)/R_0$ as a function of time. The traces are an average of 3 to 5 independent experiments. Panel b shows the relative resistance change, ((initial − final)/initial) as a function of peptide concentration. Panel c shows the averaged capacitance from the same experiments. The error bars shown at the ends of the curves are the time-averaged standard error. To determine the time constant for recovery, the curves shown in panel a were fitted to Eq. (2) as described in the Materials and methods section. The time constants are shown at the bottom right.

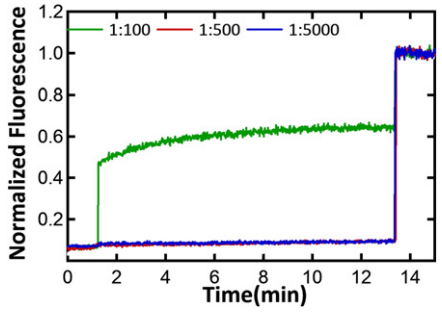

Fig. 2. Melittin-induced leakage of ANTS/DPX from POPC/Chol vesicles. The normalized ANTS fluorescence is shown as a function of time for a solution of 1 mM ANTS/DPX containing vesicles made from 75% POPC and 25% cholesterol. Melittin was added to the solution at about 1.3 min at peptide:lipid ratios of 1:100, 1:500 and 1:5000. The intensity at each point was normalized to the maximum intensity measured at about 13 min after Triton-X100 solubilization of the vesicles.

(Fig. 1c). Thus, neither the overall bilayer thickness nor the relative permittivity of the bilayers is changed significantly by melittin.

To better understand the EIS results, we performed vesicle leakage assays using vesicles of the same lipid composition as the upper leaflet of the supported bilayers, 75% POPC + 25% Chol. The vesicles were loaded with a fluorescent dye, ANTS, and a contact quencher, DPX, such that the ANTS fluorescence was quenched in the intact vesicles by the high concentration of DPX. Upon melittin addition, leakage across the bilayer was quantified by measuring the increase in ANTS fluorescence that occurs upon its release and dequenching. The time dependence of the fluorescence in these experiments is shown in Fig. 2. At the highest melittin concentration studied, P:L = 1:100, there is an initial burst of leakage, followed by a phase during which leakage slows substantially. Leakage does not reach 100%, under these conditions, consistent with results reported elsewhere: melittin does not cause 100% leakage from vesicles except when P:L is greater than 1:100 [23]. The burst phase occurs on a time scale of a few seconds, which is similar to the time of peptide partitioning into bilayers [47–49]. Considering that leakage experiments have a temporal resolution of a few seconds compared to several minutes for EIS, the time scales of vesicle leakage burst phase is indistinguishable from that of the initial drop in membrane resistance seen by EIS. After the initial burst, the leakage rate in the vesicles approaches zero, consistent with a recovery of the bilayer in the presence of melittin. The time scale of the recovery phase in the vesicle leakage experiments, around 10 min, is very similar to the time scale of the recovery phase in EIS. We propose that the same phenomenon is being observed in the two types of experiments, and that the phenomenon is not transmembrane pore formation. At lower concentrations, P:L = 1:5000, no vesicle leakage activity is observed, while in EIS an initial drop is observed followed by recovery. Differences in membrane permeabilization probably reflect the differences between the two detection systems: EIS is sensitive to the permeation of small ions that may pass through defects in the bilayer, while ANTS leakage from vesicles requires a pathway through the membrane that is larger than about 10 Å, and may require that melittin acts cooperatively, at least transiently.

To investigate the expected behavior of equilibrium transmembrane pores in our experiments, we investigated another α-helical peptide, alamethicin, that is known to form transmembrane pores in membranes under most conditions [50–52]. EIS results for alamethicin added to POPC/Chol bilayers are shown in Fig. 3. Alamethicin was added at peptide:lipid ratios that were similar to the melittin:lipid ratios used earlier. Like melittin, alamethicin caused an immediate decrease in bilayer resistance. However, unlike melittin, little or no recovery of the bilayer resistance was observed. Instead, the bilayer resistance decreased to a steady-state level that was linearly dependent on peptide:lipid ratio. At the highest peptide concentration studied, peptide:lipid = 1:200, the equilibrium bilayer resistance was less than 10% of the initial value for bilayers with alamethicin, while it was always greater than 50% of the initial value for bilayers with melittin. Furthermore, the change in resistance increases linearly with alamethicin

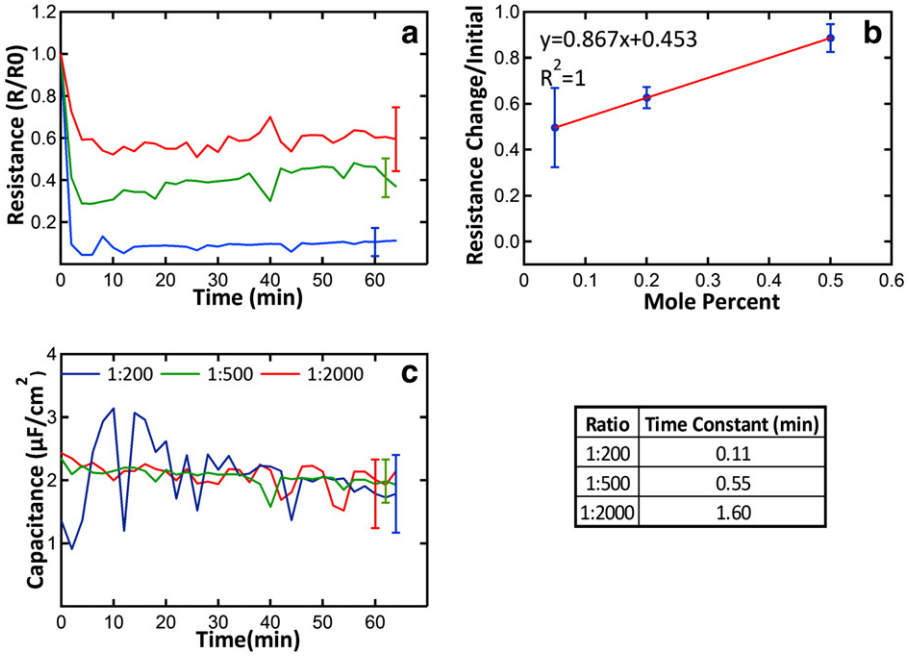

Ratio	Time Constant (min)
1:200	0.11
1:500	0.55
1:2000	1.60

Fig. 3. EIS response of POPC/Chol bilayers to alamethicin. The bilayer composition was 25% Chol, 69.1% POPC, and 5.9% DSPE-PEG2k in the lower leaflet and 75% POPC and 25% Chol in the top leaflet. Alamethicin was added in peptide to lipid ratios of 1:200, 1:1000, and 1:5000 calculated based on a final lipid concentration of 65 μM in the impedance chamber. Panel a shows the normalized change in resistance $R_m(t)/R_0$ as a function of time. The traces are an average of 3 to 5 independent experiments. Panel b shows the relative resistance change, ((initial − final)/initial) as a function of peptide concentration. Panel c shows the averaged capacitance from the same experiments. The error bars shown at the ends of the curves are the time-averaged standard error. The time constants describing the kinetics of the resistance drop are shown at the bottom right.

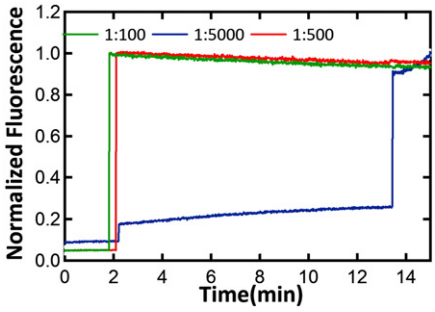

Fig. 4. Alamethicin-induced leakage of ANTS/DPX from POPC/Chol vesicles. The normalized ANTS fluorescence is shown as a function of time for a solution of 1 mM ANTS/DPX containing vesicles made from 75% POPC and 25% cholesterol. Triton-X100 was added after ~13 min to completely solubilize the vesicles.

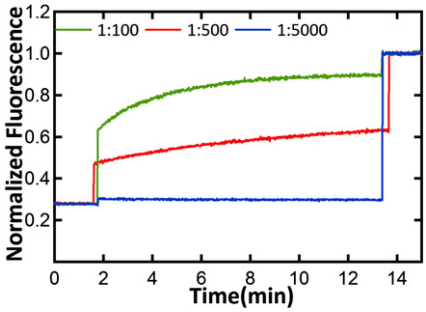

Fig. 6. Melittin-induced leakage of ANTS/DPX from POPC vesicles. Melittin was added to the solution at about 2 min at peptide:lipid ratios of 1:100, 1:500 and 1:5000. The intensity at each point was normalized to the maximum intensity measured at about 13 min after Triton-X100 solubilization of the vesicles.

concentration (Fig. 3b), as expected for a pore. As in the case of melittin, the capacitance of bilayers with alamethicin remains generally constant, indicating that the over-all bilayer architecture is unchanged.

We also performed vesicle leakage experiments using alamethicin. The leakage of ANTS/DPX from 1 mM POPC/Chol vesicles was measured for various alamethicin:lipid ratios. The results are shown in Fig. 4. Like melittin, alamethicin also causes an immediate burst of leakage. However, all but the lowest concentration (P:L = 1:5000 or ~20 peptides per vesicle) of alamethicin caused 100% leakage from vesicles, whereas no melittin concentration studied caused 100% leakage.

3.2. Pure POPC bilayers

To investigate the effect of the lipid composition on the observed behavior, we also studied the response of pure POPC bilayers to melittin. The resistance and capacitance values for POPC bilayers with melittin show a behavior that is similar to POPC/Cholesterol bilayers (Fig. 5). Except at peptide-to-lipid ratio of 1:5000, where no activity was observed, the POPC bilayers showed a rapid decrease in resistance followed by an exponential recovery that had a time constant of about 10 min. Unlike POPC/Chol bilayers, the resistance of pure POPC recovered completely to the value measured before peptide addition. Because melittin's interaction with POPC and the formation of its α-helical secondary structure in bilayers are driven by simple hydrophobic partitioning [8,9,53,54], the peptide remains associated with the bilayers as an α-helix under all conditions. Thus, the recovery of bilayer resistance requires that melittin rapidly equilibrate into an inactive, but membrane-bound state.

We also performed vesicle leakage studies with POPC bilayers and melittin (Fig. 6). The general features of the leakage from POPC vesicles were similar to those observed for POPC/Chol vesicles. There is a rapid burst of leakage, followed by a second phase during which leakage slows down. At the concentrations studied (up to P:L of 1:100) leakage stops before reaching 100%, consistent with our previously published results [21,23]. Melittin is slightly more potent in POPC compared to POPC/Chol, as also reported elsewhere [55,56]. Yet, the potency is still much lower than that of alamethicin, suggesting a similar mechanism of melittin action in POPC/Chol and pure POPC bilayers.

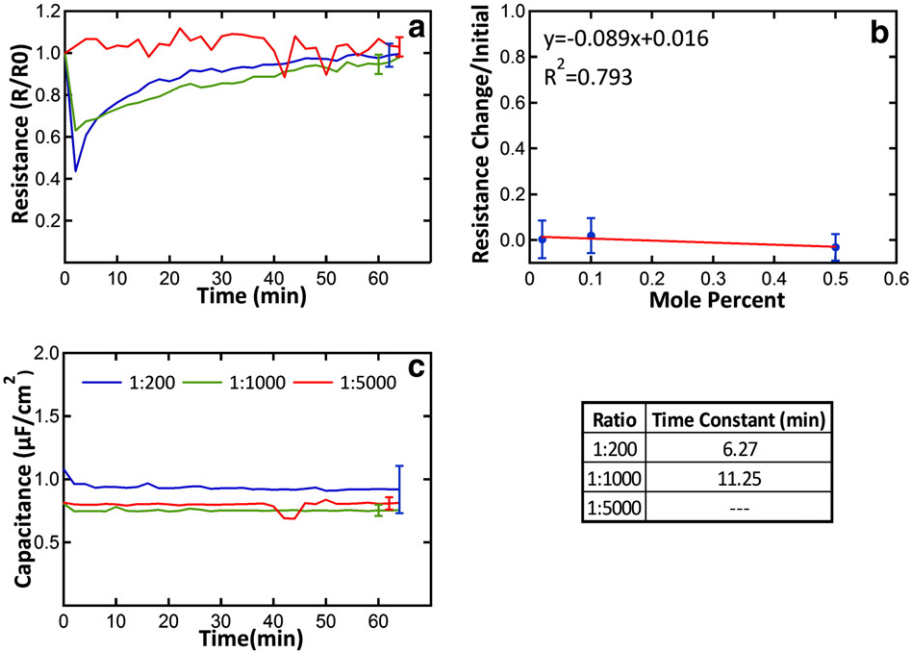

Ratio	Time Constant (min)
1:200	6.27
1:1000	11.25
1:5000	---

Fig. 5. EIS response of POPC bilayers to melittin, for different melittin to lipid ratios. The bilayer composition was 94.1% POPC and 5.9% DSPE-PEG2k in the lower leaflet and 100% POPC in the top leaflet. Panel a shows the normalized change in resistance $R_m(t)/R_0$ as a function of time. The traces are an average of 3 to 5 independent experiments. Panel b shows the relative resistance change, ((initial − final)/initial) as a function of peptide concentration. Panel c shows the averaged capacitance from the same experiments. The error bars shown at the ends of the curves are the time-averaged standard error. The time constants describing the recovery kinetics are shown at the bottom right.

3.3. POPC/POPG bilayers

We further tested the effect of melittin on POPC bilayers containing 10% anionic POPG in the upper monolayer. In Fig. 7 we show the electrical response of such bilayers to different concentrations of melittin. The initial bilayer response to melittin was similar to that of the other bilayers studied, with a drop in resistance to less than 50% of the initial value, even at the highest peptide concentration. However, in the case of POPG containing bilayers, the recovery was much slower such that the recovery was incomplete at 60 min after melittin addition.

We also performed vesicle leakage experiments with POPC/POPG vesicles (Fig. 8). The general features of the leakage were similar to the leakage observed for POPC/Chol and POPC vesicles. Again, there was a burst of leakage, followed be a second slower phase (as revealed by the slight slope at 1:500 peptide to lipid ratio) during which leakage slows. The potency of melittin in destabilizing POPC/POPG bilayers was still far lower than the potency of alamethicin for POPC/Chol destabilization.

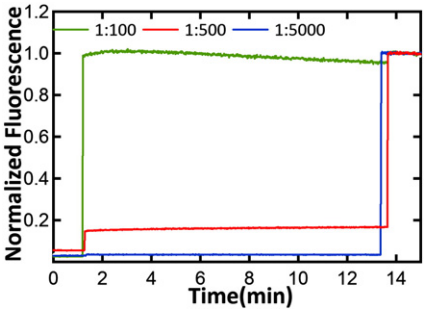

Fig. 8. Melittin-induced leakage of ANTS/DPX from POPC/POPG vesicles. The normalized ANTS fluorescence as a function of time for a solution of 1 mM ANTS/DPX containing vesicles made from 90% POPC + 10% POPG. Melittin was added to the solution at about 1.5 min at peptide:lipid ratios of 1:100, 1:500 and 1:5000. The intensity at each point was normalized to the maximum intensity measured at 13 min after Triton-X100 solubilization of the vesicles.

4. Discussion

In this work, we used electrochemical impedance spectroscopy (EIS) and vesicle leakage to study the response of lipid bilayers of various lipid compositions to the membrane permeabilizing peptide melittin at low concentration. Despite the inherent limitations of EIS (e.g. EIS only follows the movement of charged molecules and requires the assembly of a robust planar bilayer) this technique can provide unique information about the response of bilayers to low concentrations of active peptides [34]. Our goal was to use the unique sensitivity and capabilities of EIS to determine if there is evidence that melittin forms equilibrium, membrane-spanning pores. Experiments were done at controlled peptide to lipid ratios (P:L) from 1:200 down to 1:5000. At these concentrations detergent-like bilayer solubilization by melittin does not occur [23]. As the action of membrane destabilizing peptides is dependent on various experimental factors, including the lipid composition, we used three different types of bilayers in these studies: 1) plain PC bilayers, 2) PC bilayers with cholesterol, which are generally more resistant to permeabilization by melittin and other peptides [21,26,55,57], and 3) PC bilayers with anionic PG lipids, which are often more susceptible to permeabilization by cationic peptides [58–61]. All the measurements gave similar results. The melittin-dependent permeabilization of bilayers is not consistent with the formation of membrane-spanning, equilibrium pores under the conditions studied. Instead, both vesicle leakage and EIS experiments show evidence of rapid, but transient membrane permeabilization. EIS showed a transient decrease in bilayer resistance after addition of peptide. The most likely transient state is one in which the membrane-bound melittin is asymmetrically distributed across the bilayer because it is initially bound to the outer monolayer only. We speculate that leakage slows or stops once melittin has translocated and equilibrated across

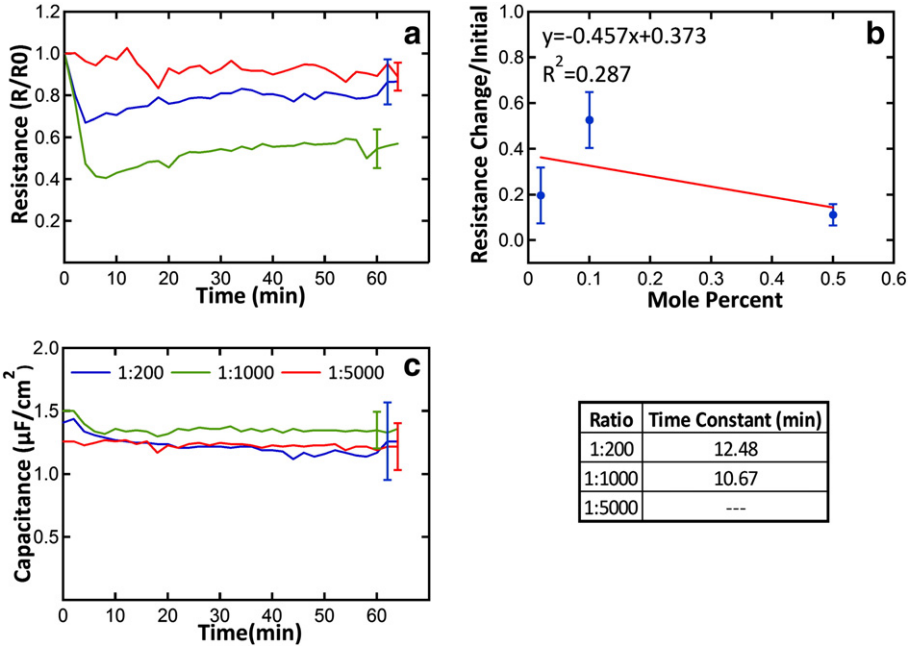

Ratio	Time Constant (min)
1:200	12.48
1:1000	10.67
1:5000	---

Fig. 7. EIS response of POPC/POPG bilayers to melittin. The bilayer composition was 94.1% POPC and 5.9% DSPE-PEG2k in the lower leaflet and 90% POPC + 10% POPG in the top leaflet. Melittin was added in peptide to lipid ratios of 1:200, 1:1000, and 1:5000 calculated based on a final lipid concentration of 65 μM in the impedance chamber. Panel a shows the normalized change in resistance $R_m(t)/R_0$ as a function of time. The traces are an average of 3 to 5 independent experiments. Panel b shows the relative resistance change, ((initial − final)/initial) as a function of peptide concentration. Panel c shows the averaged capacitance from the same experiments. The error bars shown at the ends of the curves are the time-averaged standard error. To determine the time constant for recovery, the curves shown in panel a were fitted to Eq. (1) starting at the point of lowest resistance. The time constants describing the recovery phase are shown at the bottom right.

the bilayer. In support of this idea, the final equilibrium resistance by EIS was close to the initial value and did not depend on the peptide concentration. Similarly, vesicle leakage assays showed an initial burst of leakage followed by a slow phase during which leakage stopped before the vesicles had released all of their entrapped contents. The timescales for both the fast and slow phases were similar for the two techniques, supporting the idea that both techniques are probing the same phenomena.

To verify that these techniques could recognize equilibrium transmembrane pores, we also studied the bilayer's response to the amphipathic α-helical peptide alamethicin, which is known to form such structures [51,62–64]. We found that both EIS and leakage experiments gave results for alamethicin that were consistent with equilibrium, transmembrane pores. In impedance experiments, we observed a sharp decrease in the resistance of supported bilayers to a new equilibrium value that was stable. The decrease in resistance was linearly dependent on the peptide concentration, and there was little or no recovery of bilayer resistance, which remained at a steady-state low resistance after alamethicin addition. In vesicle leakage measurements, alamethicin caused 100% leakage of probes from vesicles, with little evidence of transient/incomplete leakage events down to P:L of 1:1000. Only at P:L of 1:5000 (only 20 peptides per vesicle) did alamethicin show less than 100% leakage over the course of the 15 min experiment.

Numerical simulations have demonstrated that a single water-filled peptide pore in a large unilamellar vesicle will allow the release of all entrapped contents within a few seconds [65]. All the vesicle leakage assays discussed here show evidence of this kind of effect. After alamethicin addition, for example, essentially all of the vesicle contents are released within the first 2–3 s, except when P:L≤1:5000. The release is so rapid that we cannot capture it in the ~5 s mixing time of the vesicle leakage experiments. For melittin, there is also a very rapid burst of leakage (at least at P:L = 1:100), however unlike the case for alamethicin, only a fraction of the vesicle contents are released, and the rest remain entrapped indefinitely at this P:L. At lower P:L, we observed little leakage, consistent with published results [23,24]. Only at much higher P:L (e.g. P:L = 1:50), melittin-induced permeabilization is complete [23]. We conclude that if melittin forms transmembrane, multimeric pores in bilayers at all, it only happens in the first moments of peptide-membrane interaction and the pores are transient, not equilibrium, structures. In agreement with this conclusion, the impedance experiments report a real-time drop in bilayer resistance that occurs over the first minute or two after peptide addition. The initial timescale appears slower in impedance measurements, but this is due to the fact that data points are acquired every 2 min. In the presence of melittin, the bilayer recovers its resistance, at least partially, while for alamethicin there is no recovery. Previously published results support the contrast between melittin and alamethicin. For example, we have shown that lipid vesicles with melittin up to about P:L = 1:200 are not permeable to small molecule probes a few hours after peptide addition, while vesicles with alamethicin at P:L≤1:2000 remain permeable to small molecules indefinitely [21,23]. Furthermore it has been shown that melittin causes graded leakage from LUVs [66] and from GUVs [10] rather than all-or-none leakage as expected for equilibrium pores. Graded leakage can only occur if there is transient permeabilization [44,67].

One of the advantages of EIS is that it yields direct measurements of a peptides' effect on the bilayer resistance and capacitance even after transient events have taken place. When the melittin-bilayer system has equilibrated (~30 min), the bilayer resistance values by EIS are close to the original value, even for P:L = 1:200. For POPC bilayers, the equilibrium resistance is indistinguishable from the peptide-free bilayer, while for POPC/Chol and POPC/POPG bilayers there is a small decrease in resistance at equilibrium suggesting a slight perturbation of the bilayer barrier properties.

In summary, here we used EIS to augment standard vesicle leakage assays where the bilayer permeability properties are usually not directly measurable once leakage of entrapped analytes has taken place. The surprising observation of the studies described here was that the addition of melittin to bilayers caused only rapid, transient leakage which was quickly followed by a recovery of the bilayers permeability barrier that occurred despite the continued presence of melittin bound to the bilayers. These observations, which were made up to a peptide-to-lipid ratio of 1:200 are consistent with a model in which melittin forms an initial membrane-disrupting, non-equilibrium state upon binding to a membrane, but then reorganizes into a state that is much less disruptive to the bilayer. Mechanistic models or simulations in which melittin forms equilibrium transmembrane pores, or toroidal pores, at these sub-solubilizing concentrations are not consistent with the EIS data, or with the vesicle leakage data. Instead, permeabilization occurs through a transient process that is not well understood. We hope that future molecular dynamics simulations and additional experiments can help elucidate the structure of the transient state.

Acknowledgement

This study was supported by the NSF DMR 1003441 and NSF DMR 1003411.

References

[1] R.E. Hancock, H.G. Sahl, Antimicrobial and host-defense peptides as new anti-infective therapeutic strategies, Nat. Biotechnol. 24 (2006) 1551–1557.
[2] A. Chugh, F. Eudes, Y.S. Shim, Cell-penetrating peptides: Nanocarrier for macromolecule delivery in living cells, IUBMB Life 62 (2010) 183–193.
[3] H. Bayley, Designed membrane channels and pores, Curr. Opin. Biotechnol. 10 (1999) 94–103.
[4] C.E. Dempsey, The actions of melittin on membranes, Biochim. Biophys. Acta 1031 (1990) 143–161.
[5] T.C. Terwilliger, D. Eisenberg, The structure of melittin. II. Interpretation of the structure, J. Biol. Chem. 257 (1982) 6016–6022.
[6] B. Bechinger, Structure and functions of channel-forming peptides: magainins, cecropins, melittin and alamethicin, J. Membr. Biol. 156 (1997) 197–211.
[7] C.E. Dempsey, R. Bazzo, T.S. Harvey, I. Syperek, G. Boheim, I.D. Campbell, Contribution of proline-14 to the structure and actions of melittin, FEBS Lett. 281 (1991) 240–244.
[8] G. Schwarz, G. Beschiaschvili, Thermodynamic and kinetic studies on the association of melittin with a phospholipid bilayer, Biochim. Biophys. Acta 979 (1989) 82–90.
[9] A.S. Ladokhin, S.H. White, Folding of amphipathic α-helices on membranes: energetics of helix formation by melittin, J. Mol. Biol. 285 (1999) 1363–1369.
[10] M.T. Lee, W.C. Hung, F.Y. Chen, H.W. Huang, Mechanism and kinetics of pore formation in membranes by water-soluble amphipathic peptides, Proc. Natl. Acad. Sci. U. S. A. 105 (2008) 5087–5092.
[11] A.S. Ladokhin, S.H. White, 'Detergent-like' permeabilization of anionic lipid vesicles by melittin, Biochim. Biophys. Acta 1514 (2001) 253–260.
[12] D. Sengupta, H. Leontiadou, A.E. Mark, S.J. Marrink, Toroidal pores formed by antimicrobial peptides show significant disorder, Biochim. Biophys. Acta 1778 (2008) 2308–2317.
[13] L. Yang, T.A. Harroun, T.M. Weiss, L. Ding, H.W. Huang, Barrel-stave model or toroidal model? A case study on melittin pores, Biophys. J. 81 (2001) 1475–1485.
[14] G. Kokot, M. Mally, S. Svetina, The dynamics of melittin-induced membrane permeability, Eur. Biophys. J. 41 (2012) 461–474.
[15] D. Allende, S.A. Simon, T.J. McIntosh, Melittin-induced bilayer leakage depends on lipid material properties: evidence for toroidal pores, Biophys. J. 88 (2005) 1828–1837.
[16] K.P. Santo, M.L. Berkowitz, Difference between magainin-2 and melittin assemblies in phosphatidylcholine bilayers: results from coarse-grained simulations, J. Phys. Chem. B 116 (2012) 3021–3030.
[17] S.J. Irudayam, M.L. Berkowitz, Binding and reorientation of melittin in a POPC bilayer: Computer simulations, Biochim. Biophys. Acta 1818 (2012) 2975–2981.
[18] B.G. van den, J.V. Guzman, J.T. Mika, B. Poolman, On the mechanism of pore formation by melittin, J. Biol. Chem. 283 (2008) 33854–33857.
[19] S. Frey, L.K. Tamm, Orientation of melittin in phospholipid bilayers: a polarized attenuated total reflection infrared study, Biophys. J. 60 (1991) 922–930.
[20] K. Hristova, C.E. Dempsey, S.H. White, Structure, location, and lipid perturbations of melittin at the membrane interface, Biophys. J. 80 (2001) 801–811.
[21] A.J. Krauson, J. He, W.C. Wimley, Gain-of-function analogues of the pore-forming peptide melittin selected by orthogonal high-throughput screening, J. Am. Chem. Soc. 134 (2012) 12732–12741.
[22] M. Gordon-Grossman, H. Zimmermann, S.G. Wolf, Y. Shai, D. Goldfarb, Investigation of model membrane disruption mechanism by melittin using pulse electron paramagnetic resonance spectroscopy and cryogenic transmission electron microscopy, J. Phys. Chem. B 116 (2012) 179–188.

[23] A.J. Krauson, J. He, W.C. Wimley, Determining the mechanism of membrane permeabilizing peptides: Identification of potent, equilibrium pore-formers, Biochim. Biophys. Acta 1818 (2012) 1625–1632.
[24] A.S. Ladokhin, M.E. Selsted, S.H. White, Sizing membrane pores in lipid vesicles by leakage of co-encapsulated markers: pore formation by melittin, Biophys. J. 72 (1997) 1762–1766.
[25] R.Z. Sabirov, S.V. Krasilnikov, S.V. Merkulova, E.G. Kostrzhevskaya, N.V. Shcherbaiskaya, The effect of anions on the hemolytic activity of melittin, Ukrainian Biochem. J. 62 (1990) 87–91.
[26] A. Ramamoorthy, D.K. Lee, T. Narasimhaswamy, R.P. Nanga, Cholesterol reduces pardaxin's dynamics-a barrel-stave mechanism of membrane disruption investigated by solid-state NMR, Biochim. Biophys. Acta 1798 (2010) 223–227.
[27] K.J. Hallock, D.K. Lee, J. Omnaas, H.I. Mosberg, A. Ramamoorthy, Membrane composition determines pardaxin's mechanism of lipid bilayer disruption, Biophys. J. 83 (2002) 1004–1013.
[28] A. Ramamoorthy, S. Thennarasu, D.K. Lee, A. Tan, L. Maloy, Solid-state NMR investigation of the membrane-disrupting mechanism of antimicrobial peptides MSI-78 and MSI-594 derived from magainin 2 and melittin, Biophys. J. 91 (2006) 206–216.
[29] B. Bechinger, K. Lohner, Detergent-like actions of linear amphipathic cationic antimicrobial peptides, Biochim. Biophys. Acta 1758 (2006) 1529–1539.
[30] S. Toraya, K. Nishimura, A. Naito, Dynamic structure of vesicle-bound melittin in a variety of lipid chain lengths by solid-state NMR, Biophys. J. 87 (2004) 3323–3335.
[31] T.K. Rostovtseva, C.L. Bashford, A.A. Lev, C.A. Pasternak, Triton channels are sensitive to divalent cations and protons, J. Membr. Biol. 141 (1994) 83–90.
[32] M.T. Tosteson, D.C. Tosteson, The sting. Melittin forms channels in lipid bilayers, Biophys. J. 36 (1981) 109–116.
[33] M. Pawlak, S. Stankowski, G. Schwarz, Melittin induced voltage-dependent conductance in DOPC lipid bilayers, Biochim. Biophys. Acta 1062 (1991) 94–102.
[34] J. Lin, J. Motylinski, A.J. Krauson, W.C. Wimley, P.C. Searson, K. Hristova, Interactions of membrane active peptides with planar supported bilayers: an impedance spectroscopy study, Langmuir 28 (2012) 6088–6096.
[35] J. Lin, J. Szymanski, P.C. Searson, K. Hristova, Effect of a polymer cushion on the electrical properties and stability of surface-supported lipid bilayers, Langmuir 26 (2010) 3544–3548.
[36] J. Lin, J. Szymanski, P.C. Searson, K. Hristova, Electrically addressable, biologically relevant surface-supported bilayers, Langmuir 26 (2010) 12054–12059.
[37] W.K. Chang, W.C. Wimley, P.C. Searson, K. Hristova, M. Merzlyakov, Characterization of antimicrobial peptide activity by electrochemical impedance spectroscopy, Biochim. Biophys. Acta 1778 (2008) 2430–2436.
[38] J. Lin, M. Merzlyakov, K. Hristova, P.C. Searson, Impedance spectroscopy of bilayer membranes on single crystal silicon, Biointerphases 3 (2008) FA33.
[39] V. Nikolov, J. Lin, M. Merzlyakov, K. Hristova, P.C. Searson, Electrical measurements of bilayer membranes formed by Langmuir–Blodgett deposition on single-crystal silicon, Langmuir 23 (2007) 13040–13045.
[40] V. Nikolov, A. Radisic, K. Hristova, P.C. Searson, Bias-dependent admittance in hybrid bilayer membranes, Langmuir 22 (2006) 7156–7158.
[41] E. Li, M. Merzlyakov, J. Lin, P. Searson, K. Hristova, Utility of surface-supported bilayers in studies of transmembrane helix dimerization, J. Struct. Biol. 168 (2009) 53–60.
[42] H. Sahalov, B. O'Brien, K.J. Stebe, K. Hristova, P.C. Searson, Influence of applied potential on the impedance of alkanethiol SAMs, Langmuir 23 (2007) 9681–9685.
[43] M.L. Wagner, L.K. Tamm, Tethered polymer-supported planar lipid bilayers for reconstitution of integral membrane proteins: silane-polyethyleneglycol-lipid as a cushion and covalent linker, Biophys. J. 79 (2000) 1400–1414.
[44] A.S. Ladokhin, W.C. Wimley, K. Hristova, S.H. White, Mechanism of leakage of contents of membrane vesicles determined by fluorescence requenching, Methods Enzymol. 278 (1997) 474–486.
[45] K. Hristova, M.E. Selsted, S.H. White, Interactions of monomeric rabbit neutrophil defensins with bilayers: comparison with dimeric human defensin HNP-2, Biochemistry 35 (1996) 11888–11894.
[46] W.C. Wimley, M.E. Selsted, S.H. White, Interactions between human defensins and lipid bilayers: evidence for the formation of multimeric pores, Protein Sci. 3 (1994) 1362–1373.
[47] A. Pokorny, P.F. Almeida, Kinetics of dye efflux and lipid flip-flop induced by delta-lysin in phosphatidylcholine vesicles and the mechanism of graded release by amphipathic, alpha-helical peptides, Biochemistry 43 (2004) 8846–8857.
[48] W.C. Wimley, K. Hristova, A.S. Ladokhin, L. Silvestro, P.H. Axelsen, S.H. White, Folding of β-sheet membrane proteins: a hydrophobic hexapeptide model, J. Mol. Biol. 277 (1998) 1091–1110.
[49] S.M. Gregory, A. Cavenaugh, V. Journigan, A. Pokorny, P.F. Almeida, A quantitative model for the all-or-none permeabilization of phospholipid vesicles by the antimicrobial peptide cecropin A, Biophys. J. 94 (2008) 1667–1680.
[50] D.S. Cafiso, Alamethicin: a peptide model for voltage gating and protein-membrane interactions, Annu. Rev. Biophys. Biomol. Struct. 23 (1994) 141–165.
[51] K. He, S.J. Ludtke, D.L. Worcester, H.W. Huang, Neutron scattering in the plane of membranes: structure of alamethicin pores, Biophys. J. 70 (1996) 2659–2666.
[52] K. He, S.J. Ludtke, W.T. Heller, H.W. Huang, Mechanism of alamethicin insertion into lipid bilayers, Biophys. J. 71 (1996) 2669–2679.
[53] G. Klocek, T. Schulthess, Y. Shai, J. Seelig, Thermodynamics of melittin binding to lipid bilayers. Aggregation and pore formation, Biochemistry 48 (2009) 2586–2596.
[54] E. Kuchinka, J. Seelig, Interaction of melittin with phosphatidylcholine membranes. Binding isotherm and lipid head-group conformation, Biochemistry 28 (1989) 4216–4221.
[55] H. Raghuraman, A. Chattopadhyay, Cholesterol inhibits the lytic activity of melittin in erythrocytes, Chem. Phys. Lipids 134 (2005) 183–189.
[56] H. Raghuraman, A. Chattopadhyay, Interaction of melittin with membrane cholesterol: a fluorescence approach, Biophys. J. 87 (2004) 2419–2432.
[57] F. Nicol, S. Nir, F.C. Szoka Jr., Effect of cholesterol and charge on pore formation in bilayer vesicles by a pH-sensitive peptide, Biophys. J. 71 (1996) 3288–3301.
[58] W.C. Wimley, K. Hristova, Antimicrobial peptides: successes, challenges and unanswered questions, J. Membr. Biol. 239 (2011) 27–34.
[59] R.F. Epand, W.L. Maloy, A. Ramamoorthy, R.M. Epand, Probing the "charge cluster mechanism" in amphipathic helical cationic antimicrobial peptides, Biochemistry 49 (2010) 4076–4084.
[60] K. Matsuzaki, Control of cell selectivity of antimicrobial peptides, Biochim. Biophys. Acta 1788 (2008) 1687–1692.
[61] Z. Jiang, A.I. Vasil, J. Hale, R.E. Hancock, M.L. Vasil, R.S. Hodges, Effects of net charge and the number of positively charged residues on the biological activity of amphipathic alpha-helical cationic antimicrobial peptides, Biopolymers 90 (2008) 364–383.
[62] S. Qian, W. Wang, L. Yang, H.W. Huang, Structure of the alamethicin pore reconstructed by X-ray diffraction analysis, Biophys. J. 94 (2008) 3512–3522.
[63] H.W. Huang, Y. Wu, Lipid-Alamethicin Interactions Influence Alamethicin Orientation, Biophys. J. 60 (1991) 1079–1087.
[64] K. Hristova, W.C. Wimley, V.K. Mishra, G.M. Anantharamiah, J.P. Segrest, S.H. White, An amphipathic α-helix at a membrane interface: a structural study using a novel X-ray diffraction method, J. Mol. Biol. 290 (1999) 99–117.
[65] W.C. Wimley, Describing the mechanism of antimicrobial peptide action with the interfacial activity model, ACS Chem. Biol. 5 (2010) 905–917.
[66] S. Rex, G. Schwarz, Quantitative studies on the melittin-induced leakage mechanism of lipid vesicles, Biochemistry 37 (1998) 2336–2345.
[67] S.M. Gregory, A. Pokorny, P.F. Almeida, Magainin 2 revisited: a test of the quantitative model for the all-or-none permeabilization of phospholipid vesicles, Biophys. J. 96 (2009) 116–131.